ELSEVIER

Thermochimica Acta 391 (2002) 197–217

thermochimica acta

www.elsevier.com/locate/tca

Enthalpy relaxation in polyvinyl acetate

John M. Hutchinson*, P. Kumar

Department of Engineering, University of Aberdeen, King's College, Aberdeen AB24 3UE, UK

Received 1 October 2001; accepted 12 December 2001

Abstract

The enthalpy relaxation of polyvinyl acetate (PVAc) annealed for times up to 2000 h or so at 30 °C, some 10 K below T_g for a cooling rate of 10 K min^{-1}, has been studied by differential scanning calorimetry (DSC). The data have been analysed by the peak-shift method, and a value for the nonlinearity parameter $x = 0.44 \pm 0.02$ has been obtained. From DSC scans at 10 K min^{-1} following cooling at various rates through the transition region, the apparent activation energy and non-exponentiality parameter have been evaluated, respectively, as $\Delta h^* = 805$ kJ mol^{-1} and $0.456 < \beta < 0.6$. These relaxation parameter values are compared with others reported in the literature, and any discrepancies are discussed in terms of differences in experimental procedure and/or data analysis. Furthermore, the equilibrium enthalpic state is examined in some detail, and in particular it is argued that the equilibrium enthalpy loss at this annealing temperature of 30 °C is consistent with an extrapolation of the equilibrium enthalpy from above T_g, albeit with a slight curvature in the enthalpy–temperature equilibrium line. This is in contrast to results obtained by some other workers, where isothermal relaxation data are analysed using the Cowie–Ferguson equation and yield equilibrium enthalpy losses significantly less than those anticipated from an extrapolation. These discrepancies are discussed in terms of the nonlinearity of the relaxation process.

Keywords: Enthalpy relaxation; Polyvinyl acetate; Peak-shift method; Physical ageing

1. Introduction

The formation of a glass by cooling at constant rate from the equilibrium liquid is manifest in dilatometric and calorimetric measurements by a change in slope of the volume–temperature (*V–T*) and enthalpy–temperature (*H–T*) plots, respectively. Such plots allow the usual determination of the glass transition temperature, T_g, as the temperature at which the high-temperature (liquid) and low-temperature (glassy) asymptotes to the *V–T* and/or *H–T* curves intersect. This temperature depends on the cooling rate because the departure, on cooling, from the equilibrium liquid asymptote occurs when the timescale for molecular motions within the glass-forming liquid begins to become longer than the time available for such motions, which is determined by the cooling rate. This so-called ''freezing-in'' process occurs over a certain temperature interval, typically some 15–20 K wide, centred on T_g.

If the cooling is arrested within the glassy regime and the temperature held constant at an annealing temperature T_a, a process of volume or enthalpy relaxation, or more generally of structural relaxation or physical ageing [1–3], will occur isothermally as the non-equilibrium glass seeks to attain a lower energy equilibrium liquid-like state. For most polymer

* Corresponding author. Tel.: +44-1224-272791; fax: +44-1224-272497.
E-mail address: j.m.hutchinson@eng.abdn.ac.uk (J.M. Hutchinson).

0040-6031/02/$ – see front matter
PII: S0040-6031(02)00184-3

glasses, the attainment of equilibrium can be achieved, within reasonable experimental timescales, only in a limited temperature interval for T_a down to some 10 or 15 K below the T_g for a cooling rate of, say, 20 K min^{-1}. Indeed, this interval can be even narrower, particularly for enthalpy relaxation, which has been reported by various authors [4–6] to occur more slowly than volume relaxation, in several different polymers. For this last reason, and because in volume relaxation the volume is measured directly whereas in enthalpy relaxation the enthalpy is (usually) only measured indirectly, dilatometry offers some advantages over differential scanning calorimetry (DSC) for the study of isothermal structural relaxation.

Many years ago, Kovacs [7] made an extensive study of the volume relaxation behaviour of glassy polymers. One observation from this work was that the measured equilibrium values of the volume following isothermal relaxation at various T_a below $T_g(q_1)$, the glass transition temperature corresponding to the experimental cooling rate q_1, fell on an extrapolation of the equilibrium values of volume measured at various temperatures above T_g. Though not explicitly stated in other dilatometric studies, the same observation has been made repeatedly [6,8–10]. The extrapolation is invariably an excellent linear one, implying that the coefficient of cubical expansion of the equilibrium liquid is sensibly constant over the temperature range involved.

On the other hand, the equivalent observation in respect of enthalpy relaxation is not universally accepted. Indeed, there is a growing body of work which suggests that the extrapolation of equilibrium values of the enthalpy from the liquid-like state above T_g to annealing temperatures T_a below $T_g(q_1)$ is unreliable. Notable in this respect is the approach of Cowie and Ferguson (CF) and co-workers [11–14], who use a semi-empirical function:

$$\Delta H(t_a) = \Delta H_\infty \left[1 - \exp\left\{-\left(\frac{t_a}{\tau}\right)^\beta\right\}\right] \quad (1)$$

to describe the ageing time (t_a) dependence of the relaxed enthalpy (ΔH) relative to the unaged state. In equilibrium, the relaxed enthalpy reaches its limiting constant value ΔH_∞, and the equation takes the form of a stretched exponential with exponent $\beta\,(0 \leq \beta \leq 1)$ and characteristic time τ. By fitting Eq. (1) to experimental data, it is possible to extract values of ΔH_∞, which are invariably much less than the linearly extrapolated values, denoted by ΔH^*_∞ and given by $\Delta H^*_\infty = \Delta C_p\,\Delta T$, where ΔC_p is the difference between the specific heat capacities of the equilibrium liquid (C_{pl}) and of the asymptotic glass (C_{pg}), and ΔT the difference between the fictive temperature of the unaged glass (equal to the glass transition temperature) and the ageing temperature T_a.

Such analysis and observations have prompted the idea of a new configurational entropy model [15–18] for enthalpy relaxation, in which the limit state for isothermal relaxation need not necessarily be identified with an extrapolation of equilibrium enthalpies from higher temperatures. This interesting concept is in clear contrast to the observations from volume relaxation experiments, discussed above [6–10], and demands closer scrutiny. There are, in this respect, several "pitfalls" to be avoided [9].

First, whilst the cubical thermal expansion coefficient of most glassy polymers is rather constant in a reasonably wide temperature interval around T_g, implying a valid linear extrapolation of V–T data, the specific heat capacity usually shows a significant temperature dependence. This would require a non-linear extrapolation of H–T data, with an upward curvature since C_p usually increases with increasing temperature, which would lead to extrapolated values of ΔH_∞ less than those (ΔH^*_∞) defined by the linear extrapolation.

Second, the common observation that enthalpy relaxation occurs more slowly than volume relaxation means that an equilibrium enthalpic state is achieved during isothermal ageing below $T_g(q_1)$ considerably more rarely than is the analogous equilibrium volumetric state at an equivalent temperature. Furthermore, since the relaxed enthalpies are indirect rather than direct measurements, there is an additional uncertainty regarding the achievement of equilibrium.

An immediate consequence of the above is that ΔH_∞ values are in large part obtained by extrapolation of isothermal relaxation data using Eq. (1), which serves to highlight the third "pitfall". Eq. (1) is a semi-empirical equation designed to fit data, which it does remarkably well. However, it has been argued [19] that this approach can be misleading, since it ignores the generally accepted requirement, which dates back over 50 years to the pioneering work of Tool [20], that the relaxation time(s), or the

characteristic time τ in Eq. (1), should not be constant during isothermal relaxation, but should increase as the relaxed enthalpy increases. Under these circumstances, the values of ΔH_∞ derived by means of fitting Eq. (1) to experimental data would not be expected to be reliable, and it would be inappropriate therefore to base new concepts upon ΔH_∞ values thus determined.

In this paper, we address the last two of these "pitfalls", in particular, by annealing polyvinyl acetate samples at a temperature T_a close to $T_g(q_1)$ for sufficiently long times to achieve equilibrium. A well-established theoretical approach to the analysis of the data, which includes the recognised essential features of structural recovery, allows the evaluation of a number of kinetic parameters describing the relaxation behaviour, which parameters are then compared with those obtained for other glassy polymers and by different approaches.

2. Experimental

2.1. Materials

The polyvinyl acetate (PVAc) used here (Mowilith 50, Hoechst) has a molecular weight $\bar{M}_w = 260\,000$, and is the same material that has been used in earlier dilatometric, calorimetric, dynamic mechanical and nonlinear optical measurements [6,21–23]. The dried granules were injection moulded into bars approximately 15 mm × 6 mm in cross-section and 50 mm long. One such bar was turned on a lathe into a rod of diameter 5 mm, and was then parted using a sharp tool into discs of thickness 0.5 mm approximately. These discs, of mass approximately 12 mg, were weighed on a microbalance, sealed in standard aluminium pans, and stored in a desiccator until required.

2.2. Differential scanning calorimetry

The DSC used in this work was a DSC-4 with TADS software and data station. The cell was enclosed in a dry box and dry nitrogen was used as the purge gas at a controlled flow rate. The baseline was checked daily, and adjustments made as necessary. The temperature scale was calibrated using *n*-octadecane (Alfa Chemicals, 99% purity) and indium (99.99% purity). A controlled cooling accessory was used with the block set at −30 °C in order to obtain fast controlled cooling rates (up to 80 K min^{-1}).

2.3. Annealing treatments

Prior to any annealing treatment, each sample was heated at 20 K min^{-1} to 60 °C, which is about 20 K above the glass transition temperature ($T_g(q_1 = -10\,\mathrm{K\,min^{-1}}) \approx 39\,°C$, see Section 4), and held at this temperature for approximately 3 min in order to erase its previous thermal history. It was then cooled at 10 K min^{-1} to the annealing temperature T_a, which was selected as 30 °C, i.e. approximately 10 K below $T_g(q_1 = -10\,\mathrm{K\,min^{-1}})$.

Samples which were to be annealed for times longer than 4 h were transferred, immediately after this controlled cooling, into copper tubes of 8 mm internal diameter, 1 mm wall thickness approximately, and with a flat base for good thermal contact with the sample (see Fig. 1). The tube was then partly filled with dry silica gel granules, sealed with a stopper and cling-film, and suspended in a temperature-controlled oil bath. The bath (Techne TE-8D) contained silicone oil which was stirred by the integral pump and an

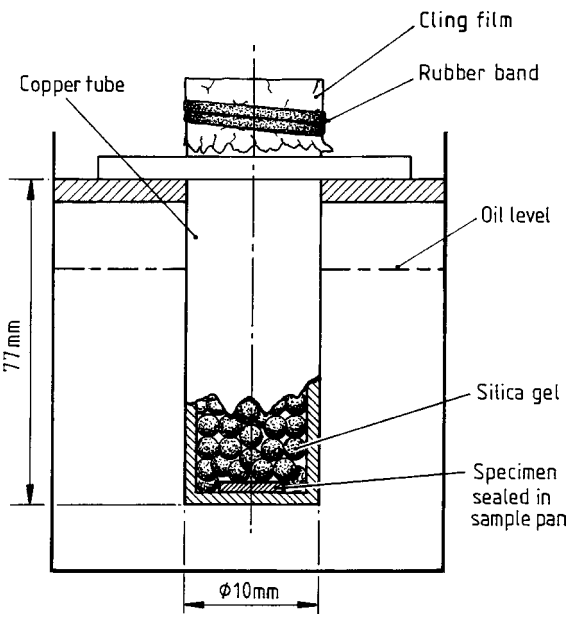

Fig. 1. Schematic illustration of copper tube containing sample for annealing in oil bath at 30 °C.

additional electrical stirrer, and the temperature was set (just above 30 °C) such that the temperature measured using a surface-contacting thermocouple probe at the interior base of each tube was 30.0 ± 0.1 °C. Because of the proximity of the annealing temperature to room temperature, a copper coil was inserted into the bath and cold water was passed through the coil at a constant rate. The bath was covered by a Perspex lid drilled with a 7 × 7 array of holes suitable for accepting the copper tubes. The identity of each sample was recorded with its location in this array, together with its date and time of entry into the bath. By using multiple samples (about 15 in total), a wide range of annealing times, up to 2000 h, could easily be achieved.

For annealing times of 4 h and less, the samples were annealed directly in the DSC. It is impractical to use the DSC as an oven for longer annealing times; furthermore, it would then not be possible to make the regular baseline checks and temperature calibrations. No discontinuity was observed between results obtained for less than and greater than 4 h, indicating that the two annealing treatments (in the oil bath and in the DSC) are equivalent.

Following the annealing treatment, the sample was returned to the DSC (if it had been annealed in the oil bath), previously set at 30 °C, cooled at 10 K min^{-1} to 5 °C, and then scanned in the DSC at a heating rate of 10 K min^{-1} up to a final temperature of 60 °C. This gave the scan for the aged sample. The sample was then immediately cooled at 10 K min^{-1} to 5 °C, and then immediately reheated up to 60 °C at a rate of 10 K min^{-1}, to give the reference scan for the unaged sample. After these two scans, the sample could be used again for further annealing times.

2.4. Controlled cooling rate experiments

A further set of experiments is required in order to determine the apparent activation energy for enthalpy relaxation and to estimate the non-exponentiality parameter. These can be obtained (see Section 3) from the dependence of the glass transition temperature (or fictive temperature) and of the endothermic peak height during the immediately subsequent heating scan, respectively, on the cooling rate through the transition region. The following procedure was therefore adopted for these experiments, the so-called constant cooling rate experiments.

A single sample was used throughout. The sample was first heated at 10 K min^{-1} to 60 °C in order to erase its previous thermal history. It was then cooled at 40 K min^{-1} to 5 °C and then immediately reheated at 10 K min^{-1} to 60 °C, the heating scan being recorded. This cycle was repeated for cooling rates of 20, 10, 5, 2.5, 1.0 and 0.5 K min^{-1}, in each case recording the heating scan from 5 to 60 °C immediately after the cooling stage. These heating scans permit the evaluation of T_g (or the fictive temperature) as a function of cooling rate, and also provide a means for estimating the width of the distribution of relaxation times, which may be characterised by the so-called non-exponentiality parameter. The use of just a single sample in these experiments is important in reducing experimental error, because the changes that are being measured, for example in T_g, are rather small.

3. Theory and data analysis

3.1. Kinetic models

It is well known that the relaxation time(s) for structural relaxation depends both on the temperature T and on the instantaneous structure of the glass. Following the early suggestion of Tool [20], it is common to quantify the structural state of the glass by the fictive temperature T_f. The partitioning of the relative contributions of temperature and structure can be effected by means of a parameter $x\,(0 \leq x \leq 1)$ [27], often referred to as the nonlinearity parameter, such that the relaxation time(s) τ may be written as

$$\tau = \tau_0 \exp\left[\frac{x\,\Delta h^*}{RT} + \frac{(1-x)\,\Delta h^*}{RT_f}\right] \quad (2)$$

where τ_0 is a reference relaxation time and Δh^* the apparent activation energy. Eq. (2) is often referred to as the Tool–Narayanaswany–Moynihan (TNM) equation in recognition of the original individual contributions [20,28,29].

It is also well known that a distribution of relaxation times is required in order to describe the relaxation kinetics; this is particularly well demonstrated, for example, by the famous memory effect experiments of Kovacs [8]. In the KAHR model [24], a discrete distribution is used, but a continuous spectrum may also

be introduced by means of the stretched exponential response function:

$$\phi(t) = \exp\left[-\left(\frac{t}{\tau}\right)^{\beta}\right] \tag{3}$$

where $\beta\,(0 \leq \beta \leq 1)$ is the non-exponentiality parameter, inversely related to the width of the spectrum.

In addition to the expressions above for the relaxation time(s) and distribution, the response of the glass is assumed to be such that it approaches the equilibrium state corresponding to its instantaneous temperature at a rate proportional to its departure from that equilibrium state. The constant of proportionality is the reciprocal of the relaxation time. Thus one may write, for the response of the glass to a heating rate $(q > 0)$ or cooling rate $(q < 0)$:

$$\frac{\mathrm{d}\delta_H}{\mathrm{d}t} = -\Delta C_p\, q - \frac{\delta_H}{\tau} \tag{4}$$

where $\delta_H = H - H_\infty$ is the excess enthalpy H relative to its value in equilibrium at that temperature, H_∞, and it is assumed that the initial state is equilibrium $(\delta_H = 0)$ at time $t = 0$.

In the KAHR model, a discrete distribution of τ is associated with discrete contributions $\delta_{H,i}$ to the total excess enthalpy δ_H, thermorheological simplicity being ensured by the dependence of each τ_i on the total δ_H rather than on the individual elements $\delta_{H,i}$. In the alternative stretched exponential approach, the assumption of a constant value for β implies thermorheological simplicity. In both cases, the response of the glass to any thermal history is completely defined by the constitutive equation (4), the TNM equation (2), and by whichever is the choice of distribution.

3.2. Peak-shift method

The basis of the peak-shift method for the evaluation of the kinetic parameters describing the relaxation (Δh^*, x and β) lies in the application of the above models to predict the response to three-step thermal cycles involving: (i) cooling at rate q_1 from equilibrium above T_g; (ii) annealing at temperature T_a for time t_a such that the excess enthalpy decreases by an amount $\bar{\delta}_H$; (iii) reheating at rate q_2 until equilibrium is again established at high temperature. The model predicts that the specific heat capacity passes through an endothermic peak at a temperature T_p, and it is the dependence of T_p on each of the experimental variables defining the three-step cycle (q_1, $\bar{\delta}_H$, q_2) which defines the peak shifts:

$$\hat{s}(q_1) = \left(\frac{\partial T_\mathrm{p}}{\partial \ln|q_1|}\right)_{\bar{\delta}_H, q_2} \tag{5}$$

$$\hat{s}(\bar{\delta}_H) = \left(\frac{\partial T_\mathrm{p}}{\partial \bar{\delta}_H}\right)_{q_1, q_2} \tag{6}$$

$$\hat{s}(q_2) = \left(\frac{\partial T_\mathrm{p}}{\partial \ln q_2}\right)_{q_1, \bar{\delta}_H} \tag{7}$$

These shifts can be normalised by defining dimensionless variables $Q_1 = \theta q_1$, $\bar{D} = \theta\bar{\delta}_H/\Delta C_p$, $Q_2 = \theta q_2$ and $T_\mathrm{p} = \theta T_\mathrm{p}$ giving normalised (dimensionless) shifts as

$$\hat{s}(Q_1) = \theta\left(\frac{\partial T_\mathrm{p}}{\partial \ln|q_1|}\right)_{\bar{\delta}_H, q_2} \tag{8}$$

$$\hat{s}(\bar{D}_H) = \Delta C_p\left(\frac{\partial T_\mathrm{p}}{\partial \bar{\delta}_H}\right)_{q_1, q_2} \tag{9}$$

$$\hat{s}(Q_2) = \theta\left(\frac{\partial T_\mathrm{p}}{\partial \ln q_2}\right)_{q_1, \bar{\delta}_H} \tag{10}$$

In these equations, θ is a temperature factor related to the apparent activation energy:

$$\theta \approx \frac{\Delta h^*}{RT_\mathrm{g}^2} \tag{11}$$

and the "hat" on $\hat{s}$ signifies that the shifts (i.e. the partial derivatives) are evaluated in limiting conditions of a "well-stabilised" glass, i.e. one which has been annealed for long times. This limiting condition is manifest as a linear relationship between T_p and any of the three experimental variables.

This last point is important because, if the glass is only "poorly stabilised" (i.e. only annealed for short times), then a different kind of endothermic peak appears, a so-called "upper peak" [30]. The difference between an upper peak and the main annealing peak lies in its dependence on the experimental conditions: in particular, the temperature T_u at which an upper peak appears is essentially independent of the amount of annealing, $\bar{\delta}_H$. The distinction between these types of endothermic peak will become clear later when the experimental data are presented.

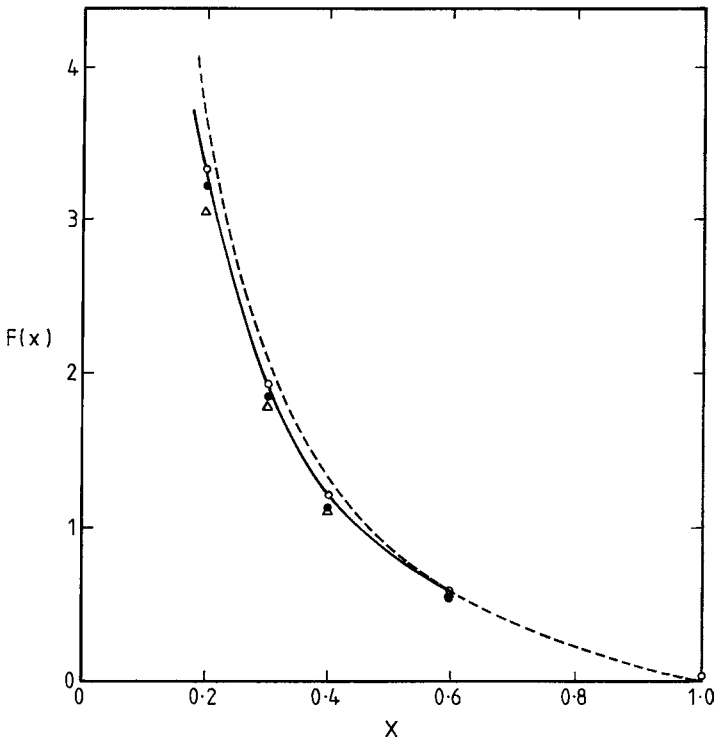

Fig. 2. Theoretical master curve for the dependence of $F(x)$ (see Eq. (12)) on x. The dependence has been evaluated for a single relaxation time (dashed line) and for three different distributions: open circles, single box discrete distribution; filled circles, double box discrete distribution; open triangles, stretched exponential response function (see Eq. (3)) with $\beta = 0.456$. Refer to Refs. [24–26] for further details.

For the main annealing peak, it can be shown [25] that the shifts are all inter-related:

$$F(x) = \hat{s}(\bar{D}_H) = \hat{s}(Q_2) - 1 = -\hat{s}(Q_1) \tag{12}$$

and their dependence on x, defined by the function $F(x)$, is remarkably sensitive, as shown by the theoretical master curve shown in Fig. 2. Furthermore, the function $F(x)$ is remarkably insensitive to the choice of distribution used (refer to caption to Fig. 2).

The experimental evaluation of $F(x)$ therefore affords a rational means for evaluating the nonlinearity parameter x, essentially independent of the distribution. This is the basis of the peak-shift method. In practice, it is most convenient to evaluate $F(x)$ from $\hat{s}(\bar{D}_H)$, i.e. from the dependence of the peak endotherm temperature on the enthalpy lost during annealing, and this is the approach adopted here. Samples of PVAc are annealed at T_a for a range of annealing times, up to 2000 h, and the peak temperature T_p for the aged sample is determined as a function of the enthalpy lost during annealing, the latter being evaluated in the usual way from the area difference between scans for the aged and unaged glasses.

3.3. Dependence of T_g on cooling rate

It can be shown, from the theories outlined above, that the glass transition temperature depends on the cooling rate q_1 according to

$$\frac{\mathrm{d}\ln|q_1|}{\mathrm{d}(1/T_g)} = -\frac{\Delta h^*}{R} \tag{13}$$

The measurement of T_g as a function of q_1 thus allows the direct evaluation of the apparent activation energy Δh^*.

In practice, it is the fictive temperature T_f that is measured during the heating scan in the DSC; for a glass reheated immediately after cooling at rate q_1, the

fictive temperature of the glass is identical to $T_g(q_1)$. The fictive temperature was determined here by the "equal area method" [31], which equates the area between the liquid-like and glassy asymptotes of the heating scan, from T_f to a temperature T_0 in the equilibrium liquid state, with the area under the heating scan and above the glassy asymptote. The apparent activation energy is found directly from a plot of log (cooling rate) versus reciprocal T_f.

The same heating scans for unannealed glasses heated in the DSC immediately after cooling at different rates through the glass transition region can be used to provide an estimate of the non-exponentiality parameter β [30]. If the curves are normalised such that C_p passes from zero to unity as the sample goes from the glassy state to the equilibrium liquid-like state on heating, then the maximum normalised value of C_p, which occurs at the upper peak[1] temperature T_u, is denoted $C_{p,u}^N$.

By comparing the experimental values of $C_{p,u}^N$ over the range of cooling rates used with values obtained from the theoretical model using various combinations of β and x, it is possible to estimate β within the limitations of the discrete values of β and x used in the modelling.

4. Results

4.1. Annealing experiments

Fig. 3 shows a selection of DSC heating scans for PVAc samples annealed at 30 °C for the times indicated. Some features are immediately apparent. First, comparing the zero annealing time (reference scan), 0.12 and 1 h annealing time curves, it can be seen that the endothermic peak temperature first decreases and then increases as t_a increases. This is a characteristic feature of short annealing time curves, and is associated with the appearance of upper peaks at short annealing times and main or annealing peaks at longer times.

[1] Note that these are, in general, upper peaks since the glasses are unannealed before reheating in the DSC. Only for the slower cooling rates, of the order of less than half the magnitude of the heating rate, does sufficient stabilisation occur during cooling for the subsequent endothermic peaks which appear on heating to be manifest as annealing or main peaks.

Second, with increasing annealing time beyond 0.12 h, the endothermic peaks grow in magnitude and move towards higher temperatures. Thus both the enthalpy loss, $\bar{\delta}_H$, and the peak temperature T_p, increase with annealing time, and Figs. 4 and 5 show that this increase is linear with $\log t_a$ until they both level off as an equilibrium state is approached at long times. By fitting straight lines to these initial linear increases, slopes of $d\bar{\delta}_H/d\log t_a = 0.98\,J\,g^{-1}$ per decade and $dT_p/d\log t_a = 2.00\,K$ per decade are obtained. The former value agrees reasonably well with other values obtained for PVAc from the data of Sharonov and Volkenshtein [32] (1.12 J g^{-1} per decade), Bair et al. [33], Wang and Filisko [34] and Cowie et al. [14] (0.88 J g^{-1} per decade), but is somewhat greater than the value found from earlier data of Cowie et al. [35] (0.78 J g^{-1} per decade).

Alternatively, the data of Figs. 4 and 5 may be represented together as a plot of T_p versus $\bar{\delta}_H$, as shown in Fig. 6. Here, instead of showing a levelling off of the data at long times as equilibrium is approached, as was seen in Figs. 4 and 5, the data points begin to cluster at the top right-hand corner of the figure as both T_p and $\bar{\delta}_H$ reach their limiting values. Thus one can see that the limiting T_p is approximately 51.7 ± 0.5 °C while the limiting $\bar{\delta}_H$ is approximately $3.75 \pm 0.25\,J\,g^{-1}$. The slope of the best-fit line to these data gives $\partial T_p/\partial\bar{\delta}_H = 2.04\,g\,kJ^{-1}$, in good agreement with the ratio of the individual slopes for T_p and $\bar{\delta}_H$ found from Figs. 4 and 5, respectively.

4.2. Evaluation of x

The evaluation of x from the master curve (Fig. 2) and using Eq. (12) with $F(x) = \hat{s}(\bar{D}_H)$ requires the prior measurement of ΔC_p (refer to Eq. (9) for the definition of $\hat{s}(\bar{D}_H)$). Here ΔC_p was measured at the fictive temperatures for several glasses formed at a range of cooling rates, and the average value was $0.505 \pm 0.010\,J\,g^{-1}\,K^{-1}$. This should be compared with literature values of $0.50\,J\,g^{-1}\,K^{-1}$ given in Table 1 of Ref. [8] and also quoted by McKinney and Simha [36], and of $0.46 \pm 0.01\,J\,g^{-1}\,K^{-1}$ measured from the C_p traces of Bair et al. [33].

Using our value for ΔC_p and the value for $\partial T_p/\partial\bar{\delta}_H$ found above, one obtains $\hat{s}(\bar{D}_H) = 1.03$. Finally, from the master curve in Fig. 2 this gives $x = 0.44 \pm 0.02$.

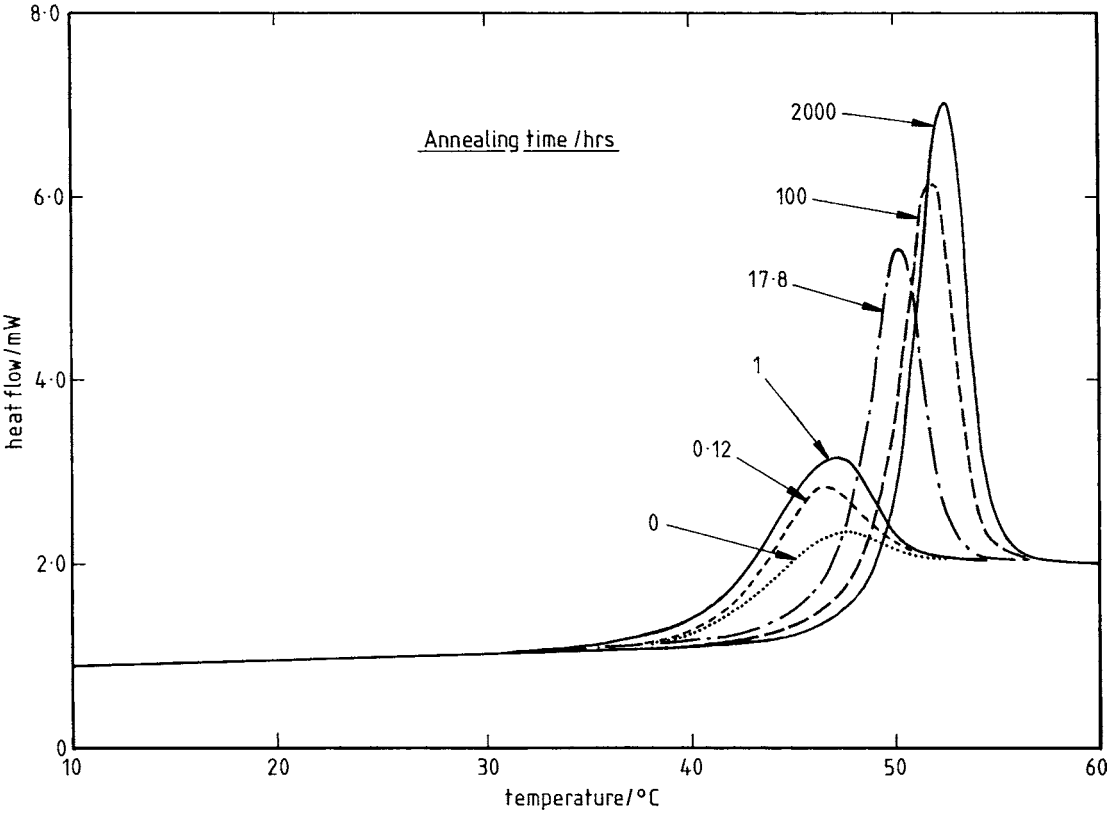

Fig. 3. Typical DSC scans, as heat flow versus temperature, for PVAc samples annealed at 30 °C for the times indicated (in hours) against each curve, following cooling at 10 K min^{-1} from equilibrium at 60 °C. The heating rate is 10 K min^{-1}.

4.3. Evaluation of Δh^*

The DSC traces for the controlled cooling rate experiments are shown in Fig. 7. The most obvious trend is of an increasingly large endothermic peak as the cooling rate decreases, which is consistent with the slower cooling rates leading to glasses of lower enthalpy, thus requiring a greater recovery of enthalpy on reheating to reach the equilibrium state again above T_g.

On closer inspection, a further characteristic feature is seen, namely that the peak endotherm temperature first decreases and then increases as the cooling rate decreases from 40 to 0.5 K min^{-1}. The explanation for this behaviour is that the nature of the peak is changing from an upper peak, observed for the fast cooling rates and hence poorly stabilised glasses, to a main or annealing peak, observed for the slow cooling rates and hence increasingly well-stabilised glasses. This is seen more clearly in Fig. 8, where the peak temperature is plotted as a function of the log (cooling rate).

To the right of the minimum, the positive slope represents the increase in the upper peak temperature T_u with increasing cooling rate q_1, and can be quantified by a normalised shift:

$$s_u(Q_1) = \theta\left(\frac{\partial T_u}{\partial \ln|q_1|}\right)_{\bar{\delta}_H=0,q_2} \tag{14}$$

where the subscript in s_u indicates an upper peak shift, in distinction to $\hat{s}$ (ref. Eqs. (5)–(10)) which represents main peak shifts. The slope of the line in Fig. 8 gives $s_u(Q_1) = 0.29$, in the calculation of which a value of $\theta = 0.99$ K^{-1} has been anticipated from the apparent activation energy (see below). This value for $s_u(Q_1)$ is similar to those found earlier [30] for two narrow fraction polystyrene samples of different molecular

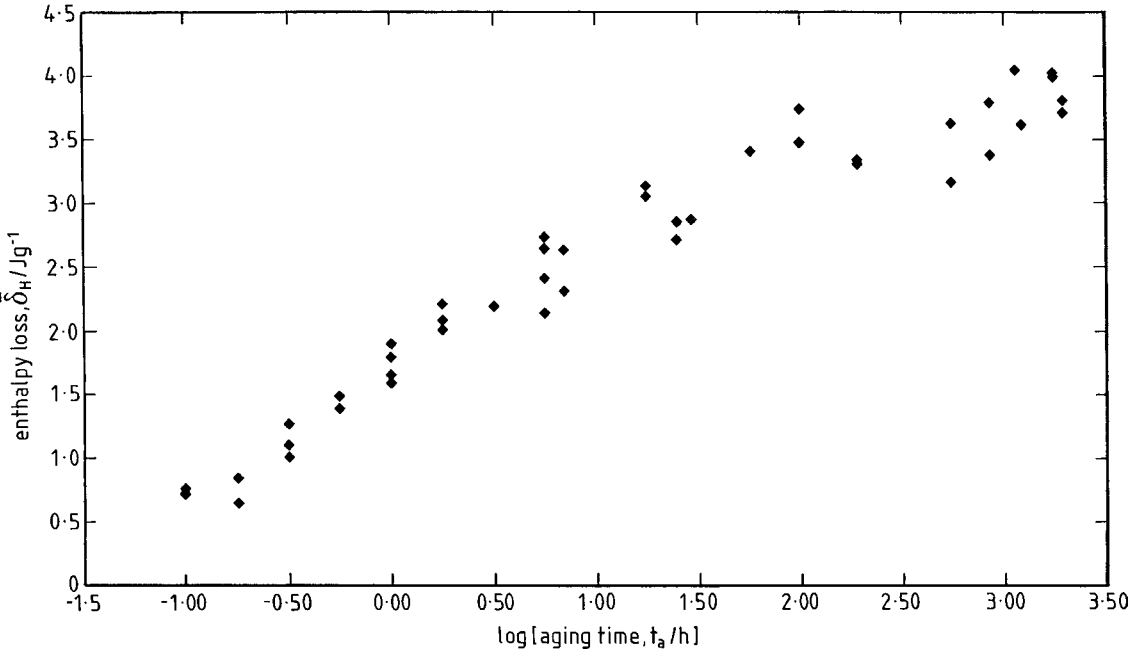

Fig. 4. Dependence of enthalpy loss, $\bar{\delta}_H$, on log (annealing time) for PVAc samples annealed at 30 °C following cooling at 10 K min^{-1} from equilibrium at 60 °C. The heating rate is 10 K min^{-1}.

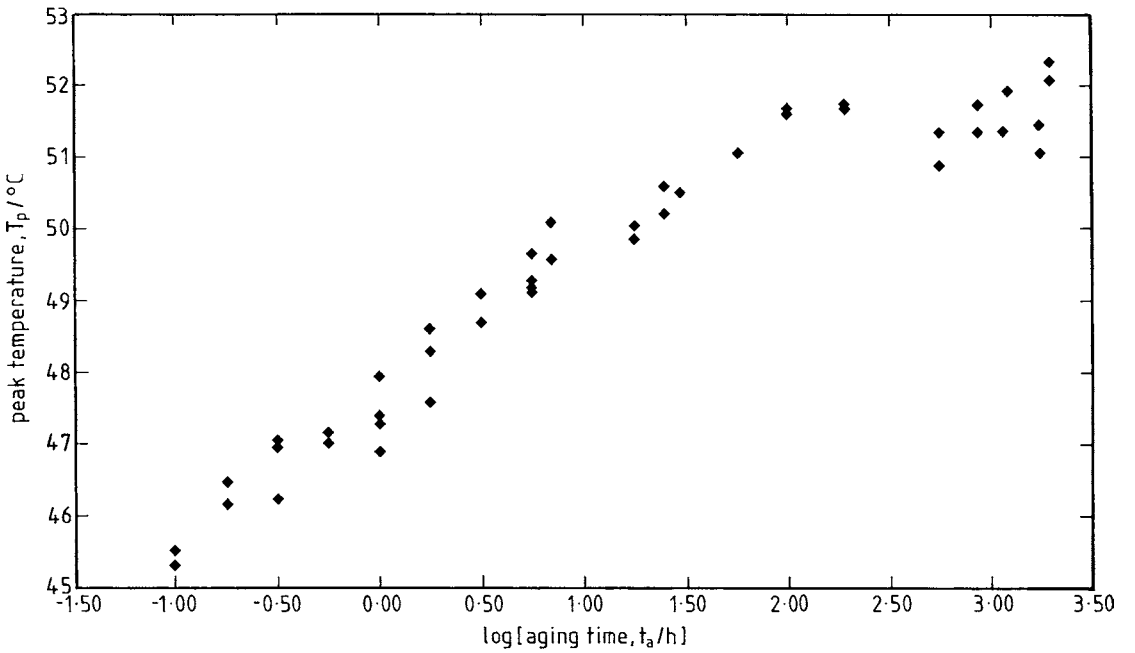

Fig. 5. Dependence of endothermic peak temperature T_p on log (annealing time) for PVAc samples annealed at 30 °C following cooling at 10 K min^{-1} from equilibrium at 60 °C. The heating rate is 10 K min^{-1}.

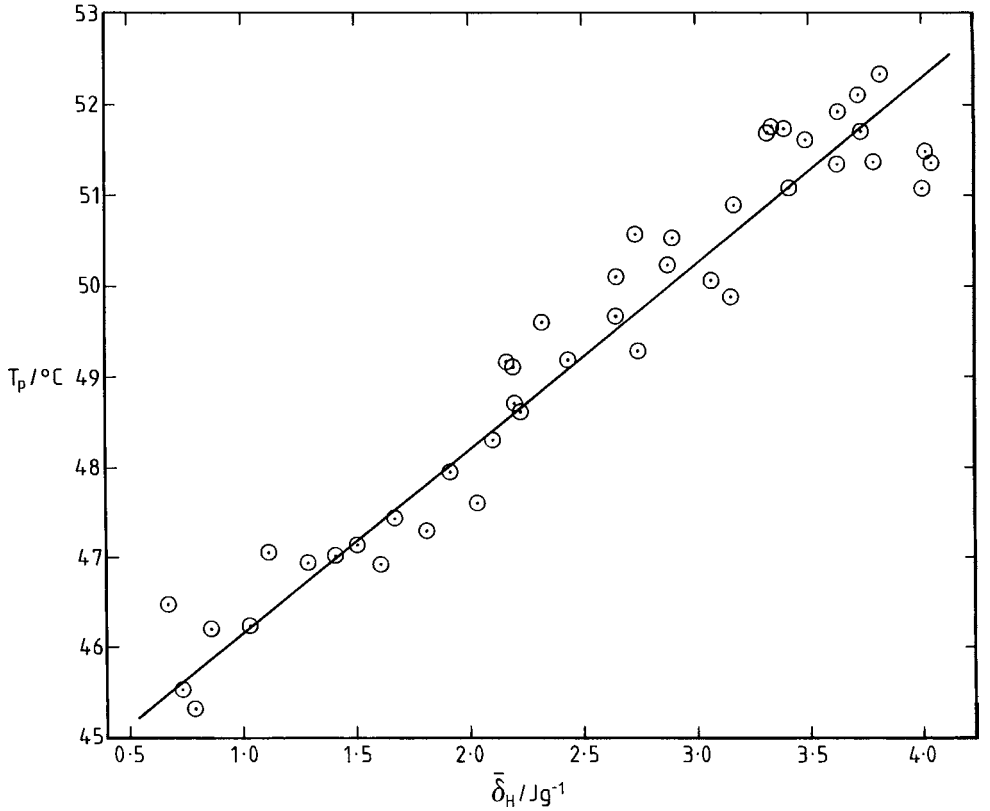

Fig. 6. Dependence of peak temperature T_p on enthalpy loss $\bar{\delta}_H$ during annealing of PVAc at 30 °C following cooling at 10 K min^{-1} from equilibrium at 60 °C. The heating rate in the DSC was 10 K min^{-1}. The full line represents a least-squares fit to the data.

weights, namely 0.18 for $\bar{M}_w = 30\,100$ and 0.22 for $\bar{M}_w = 315\,000$.

To the left of the minimum, which occurs when the cooling rate is between one-half ($q_1 = -5$ K min^{-1}) and one-quarter ($q_1 = -2.5$ K min^{-1}) of the heating rate ($q_2 = 10$ K min^{-1}), the steeply rising curve represents main peak temperatures, and indicates that the annealing peaks occur at increasing T_p as the cooling rate decreases. In the limit of very slow cooling rates, which have not been achieved here, this would become a linear relationship between T_p and $\ln|q_1|$, the slope of which is negative and defines $\hat{s}(q_1)$ (refer to Eq. (5)). It can readily be appreciated from Eq. (12) that $\hat{s}(q_1)$, and therefore also $\hat{s}(Q_1)$, must be negative. The maximum slope of this left-hand part of the curve in Fig. 8 would give a shift of $-\hat{s}(Q_1) = 0.70$ (using the same value of $\theta = 0.99$ K^{-1} as was used immediately above), which is significantly less than the value of $F(x) = 1.03$ found from $\hat{s}(\bar{D}_H)$; this simply confirms that the limiting behaviour has not been reached here at the slowest cooling rate of 0.5 K min^{-1}.

The DSC traces of Fig. 7 have been analysed by the equal area method [31] to find the fictive temperature as a function of cooling rate, and the results are shown in Fig. 9, where log (cooling rate) is plotted versus reciprocal fictive temperature. The best-fit straight line to these data yields a slope which gives $\Delta h^*/R = 96.7$ kK, hence $\Delta h^* = 805$ kJ mol^{-1}, and has a correlation coefficient of 0.9917. Taking $T_g = 311.9$ K, which is the fictive temperature for $q_1 = -10$ K min^{-1}, we can evaluate θ from Eq. (11) as $\theta = 0.99$ K^{-1}.

Other values quoted in the literature (or calculated here from published data) for the reduced apparent activation energy $\Delta h^*/R$ include the following. Using the curve-fitting approach, Sasabe and Moynihan [37]

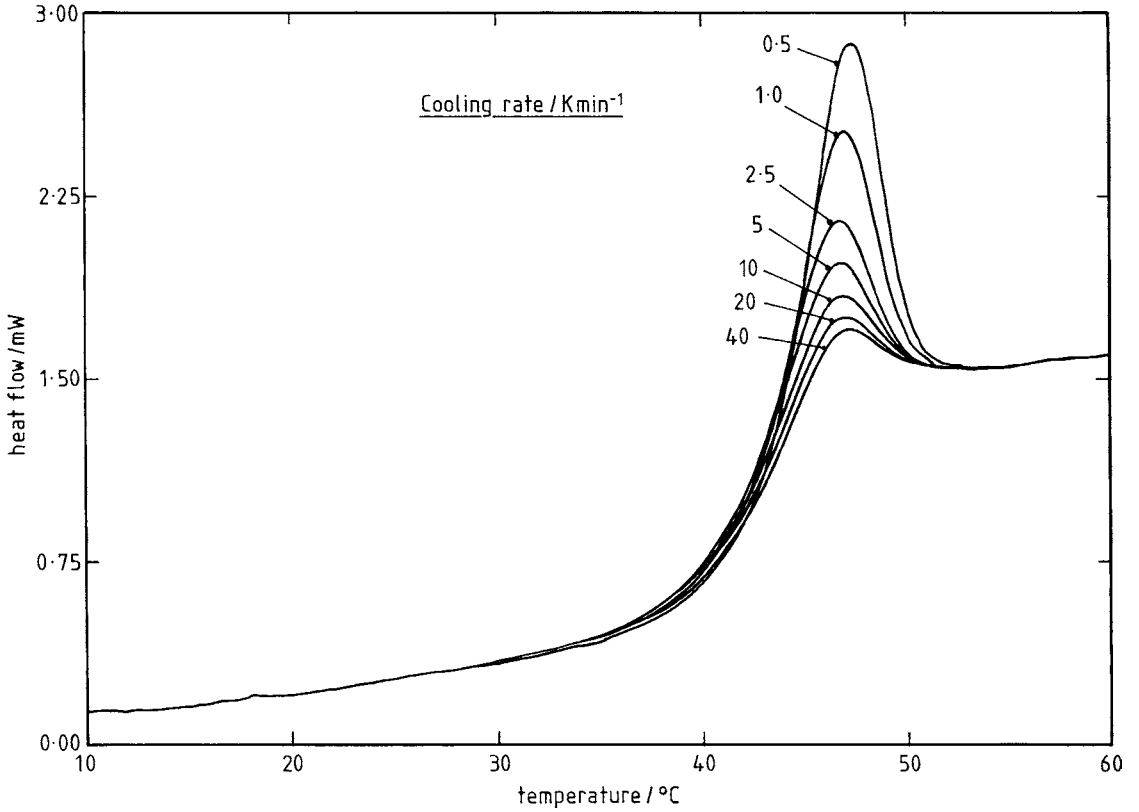

Fig. 7. DSC scans at a heating rate of 10 K min^{-1} for PVAc samples cooled at the rates indicated against each curve from equilibrium at 60 °C to a lower temperature of 5 °C and then immediately reheated.

obtain 71 kK while Hodge [38,39] quotes 88 kK ± 10%. Whilst these are reasonably close, particularly the latter, to the value obtained here, the value calculated from the data of Cowie et al. [14] (from a plot of log τ given in their Table 3 versus $1/T_a$) is only 30.7 kK; the reason for this large discrepancy is discussed further below.

4.4. Estimation of β

The same data (Fig. 7) as have been used for the evaluation of Δh^* also serve for estimating the non-linearity parameter β. The theoretical dependence of the normalised upper peak height $C^N_{p,u}$ on the logarithm of the ratio of cooling rate to heating rate in thermal cycles involving no annealing at T_a (intrinsic cycles) is shown in Fig. 10 for several combinations of β and x (see figure caption for details). The general trend of decreasing $C^N_{p,u}$ with increasing log $(|q_1|/q_2)$ is common to all of these theoretical curves, but their location is sensitive to the values of β and x. Since the value of x (=0.44) has been found above, essentially independent of the distribution, a comparison of the experimental data for $C^N_{p,u}$ with these theoretical curves allows β to be estimated within the limitation of the discrete values presented.

The experimental data are found from the magnitude of the endothermic peaks in Fig. 7 relative to the step change in heat flow measured at T_u, and are plotted together with the theoretical curves in Fig. 10. It is clear that these data also show the same general trend of decreasing $C^N_{p,u}$ with increasing log $|q_1|$. By interpolating a theoretical curve for $x = 0.44$ (the experimental value obtained above) for each value of β, it is readily apparent that the experimental data lie between those for $\beta = 0.456$ and

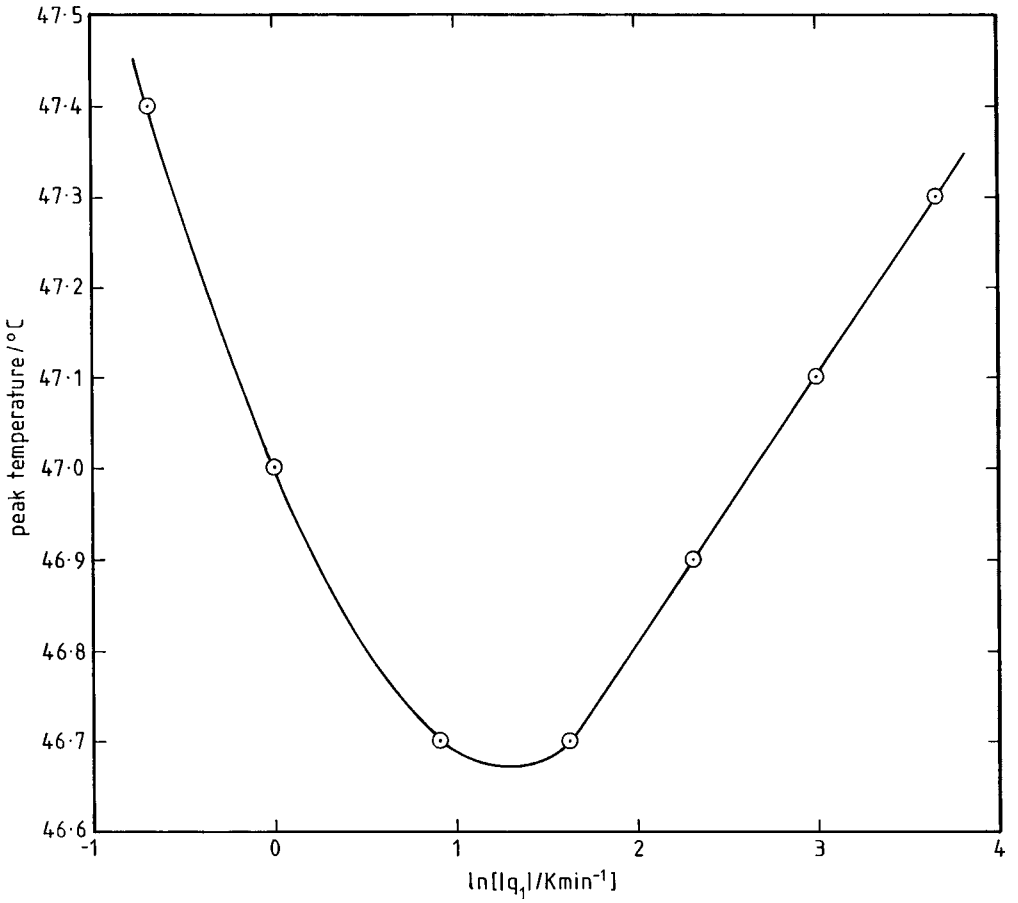

Fig. 8. Peak endotherm temperature from the DSC traces in Fig. 7 as a function of the logarithm of the absolute value of the prior cooling rate. The heating rate is 10 K min^{-1}.

0.6, and hence we may estimate that for PVAc the non-exponentiality parameter lies in the range $0.456 < \beta < 0.6$.

5. Discussion

5.1. The relaxation parameter Δh^*

These parameters have been evaluated here by the peak-shift method and, to summarise, are as follows: $\Delta h^*/R = 96.7$ kK, $\Delta h^* = 805$ kJ mol^{-1}, $x = 0.44 \pm 0.02$, $0.456 < \beta < 0.6$. It is interesting now to compare these with other values quoted in the literature for PVAc, and also to compare them with values for other polymer glasses.

Considering the apparent activation energy, we have already seen above that our value is reasonably close to those found by Sasabe and Moynihan [37] and Hodge [38,39]. In fact, it can be seen from Fig. 9, where the data of Sasabe and Moynihan are plotted together with the present data (except for one of their data points which falls outside the scale of this graph), that both form a coherent set; the difference between the values obtained for Δh^* results from the uncertainties in fitting a least-squares line to the data, these uncertainties being somewhat greater for the data of Sasabe and Moynihan than for our own. We may reasonably conclude, therefore, that $\Delta h^*/R = 97 \pm 10$ kK, and hence $\Delta h^* = 805 \pm 80$ kJ mol^{-1}.

On the other hand, as observed further above, this value is significantly higher than the value of

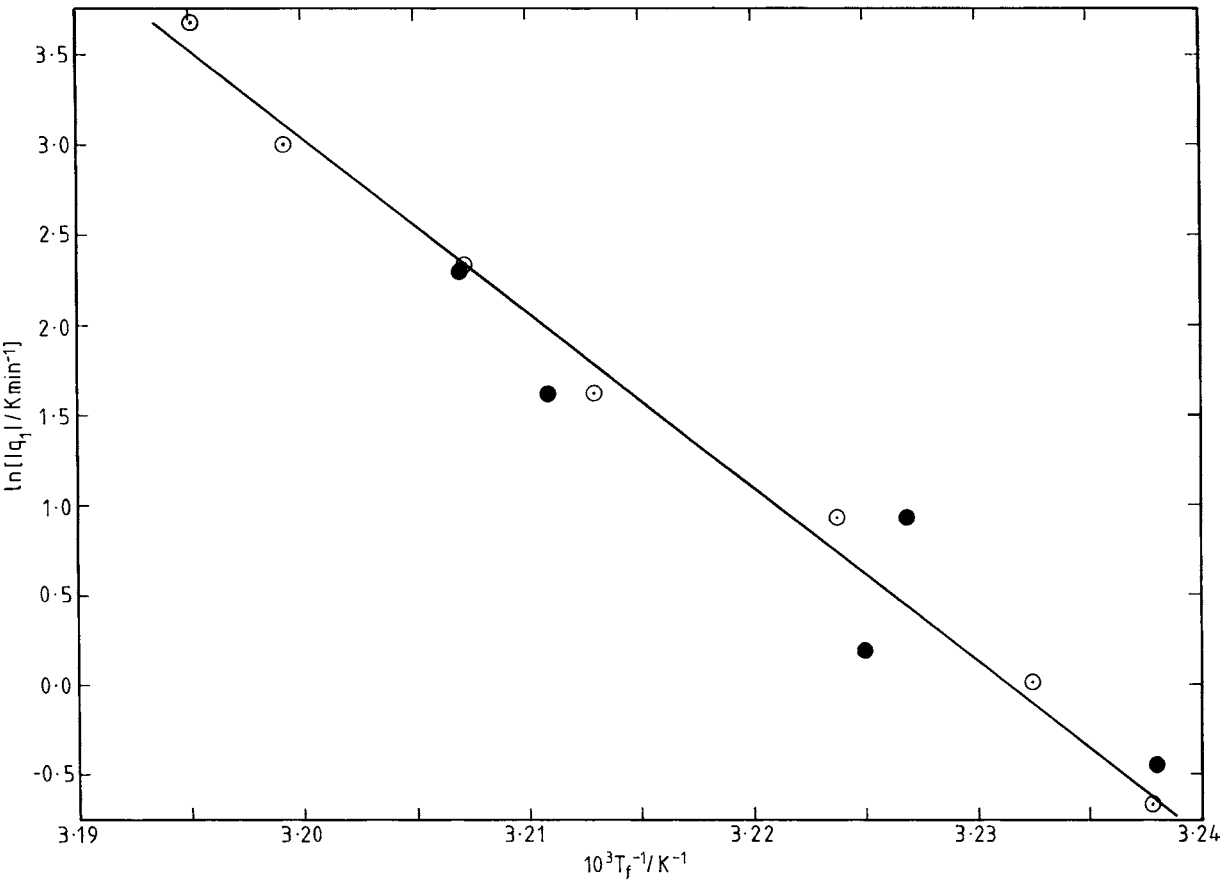

Fig. 9. Plot of ln (cooling rate) versus reciprocal fictive temperature for the constant cooling rate experiments shown in Fig. 7. The heating rate used was 10 K min^{-1}. The open circles were obtained in the present work, and the full line represents a least-squares fit to these data. The filled circles are replotted from the data of Sasabe and Moynihan [37], with one of their data points missing as it falls outside the grid.

$\Delta h^*/R = 30.7$ kK which is derived from the data of Cowie et al. [14]. We believe that this discrepancy may be explained as follows. Cowie et al. fit isothermal enthalpy relaxation data, obtained at temperatures T_a of 35, 32, 30 and 25 °C ($\Delta T = 7$, 10, 12 and 17 K, respectively, below their T_g of 42 °C), using the Cowie–Ferguson (CF) [11–14] equation (1), and from this fitting procedure they extract values of ΔH_∞, τ and β for each annealing temperature T_a. One of the problems with this approach is that the CF equation does not include one of the primary features of structural relaxation, namely that the relaxation time is dependent on the structure of the glass. Hence, any parameter values derived using the CF equation must be considered carefully, and this is discussed further immediately below.

During any isothermal relaxation, the relaxation time increases as the fictive temperature decreases (cf. Eq. (2)). If the whole relaxation process is available within the experimental timescale, as is the case for $T_a = 35$ °C, only 7 K below T_g, then the CF-calculated value of τ will be some average of the fictive temperature-dependent one. As the annealing temperature T_a is decreased, less and less of the complete relaxation is available within the experimental timescale (it is argued below that the apparent limiting values of ΔH_∞, in Fig. 4 and Table 3 of Cowie et al. [14] are not reliable). Hence the CF-calculated value of τ represents more and more the initial value of the relaxation time during the early stages of the relaxation process. In the limit, this initial value would be given by Eq. (2) with $T_f = T_g(q_1)$, where q_1 is the

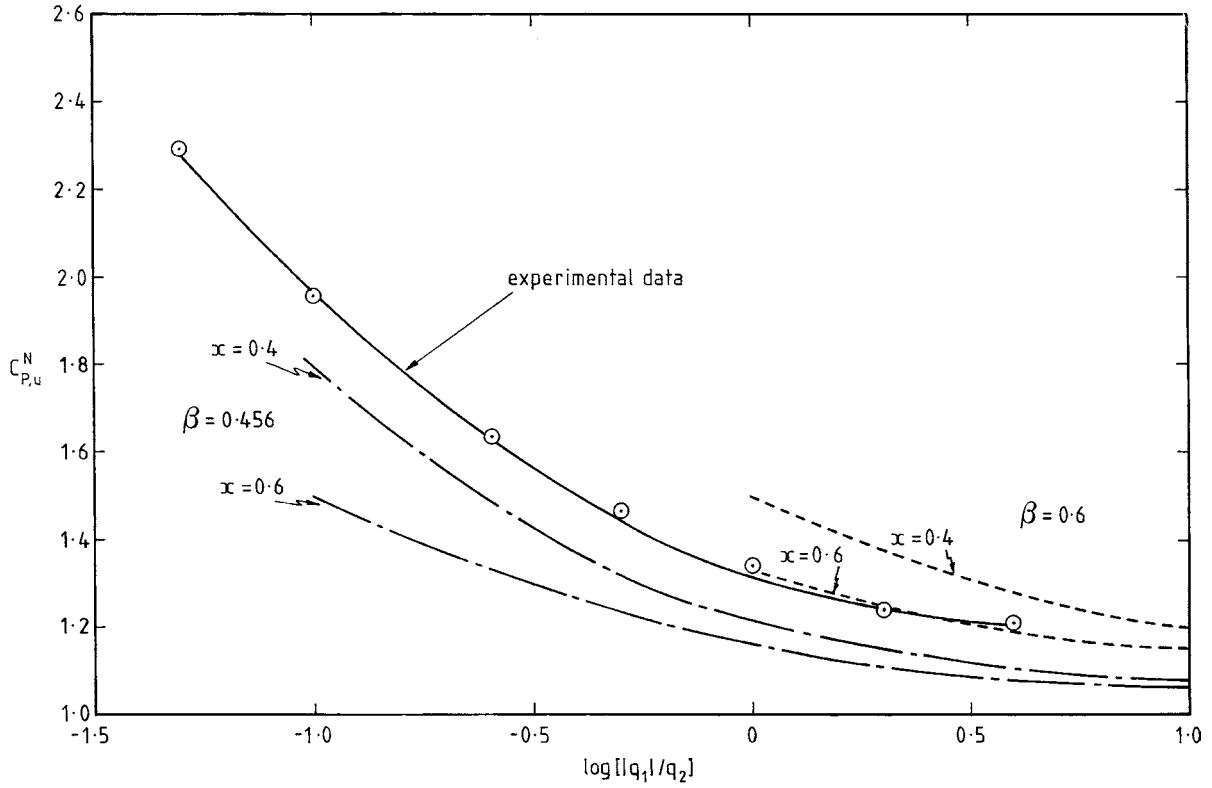

Fig. 10. Dependence of normalised upper peak height $C^{N}_{p,u}$ on log ($|q_1|/q_2$) for intrinsic thermal cycles. The experimental data are represented by the open circles, and the full line is drawn through these points to guide the eye. The theoretical curves for $\beta = 0.456$ (dash-dotted line) and $\beta = 0.6$ (dashed line) are given, each with two different values for x (0.4 and 0.6). The experimental values are obtained from the DSC traces in Fig. 7, for which the heating rate (q_2) was 10 K min^{-1}.

cooling rate used to reach the annealing temperature T_a (40 K min^{-1} in Cowie et al. [14]). Hence in the limit one would measure, from the CF-calculated values of τ as a function of T_a, a reduced apparent activation energy of $x\,\Delta h^*/R$ instead of $\Delta h^*/R$. Using our values of x and $\Delta h^*/R$, this is evaluated as 42.7 kK, closer to, but still somewhat greater than, 30.7 kK.

The continuing discrepancy lies in the fact observed above that at T_a close to T_g the CF-calculated value of τ is an averaged value, and does not approximate to the initial value. Thus, as the annealing temperature T_a is reduced, the CF-calculated value of τ becomes increasingly small, with a corresponding decrease in the apparent activation energy calculated in this way.

The same arguments can be applied to values of reduced apparent activation energy calculated by fitting the CF equation to relaxation data for other polymers. Thus, for polystyrene, the data of Brunacci et al. [13] give $\Delta h^*/R = 40$ kK (with considerable uncertainty because the relationship between log τ and T_a^{-1} is not a very good straight line) compared with 80 kK from Hodge [38,39], 70 kK from Hutchinson and Ruddy [40], and 76–110 kK from Privalko et al. [41]. Similarly, Cowie and Ferguson [11,12] find $\Delta h^*/R = 83$ kK for polymethyl methacrylate compared with 138 kK according to Hodge [39], 150 kK according to Tribone et al. [42] and 115 kK according to Hutchinson [43].

5.2. The relaxation parameter β

The range of values within which the non-exponentiality parameter β is estimated to lie from the present data, namely between 0.456 and 0.6, includes the values obtained earlier by both Sasabe and Moynihan [37] ($\beta = 0.51$) and Hodge [39] ($\beta = 0.51$).

There is therefore good agreement between these results. On the other hand, the values of β found by Cowie et al. [14] by fitting the CF equation are somewhat lower, in the range 0.33–0.45. Furthermore, their values of β depend on T_a, with a tendency to decrease as T_a decreases. These differences can be explained in terms of the omission of the nonlinearity parameter x from the CF equation, as follows.

The effect of the dependence of the relaxation time τ on the fictive temperature T_f, in other words the effect of nonlinearity, is to increase τ as T_f decreases during the isothermal approach to equilibrium. This lengthens the timescale of the isothermal relaxation process, leading to self-retarding behaviour [8]. In the CF equation, which omits this dependence of τ, the experimentally observed self-retardation must be modelled only by the effect of β. Thus, in the absence of x, the stretching exponent β must be smaller in order to model the lengthened timescale. Furthermore, the lower the annealing temperature T_a, the greater is the departure from equilibrium, and hence the greater is the effect of nonlinearity. Thus, ignoring the effect of nonlinearity becomes more pronounced as T_a decreases, and in the CF equation must be modelled by decreasing β.

5.3. The relaxation parameter x

The present value of $x = 0.44 \pm 0.02$ has been obtained by the peak-shift method. In the earlier work of Sasabe and Moyihan [37] and Hodge [39], the curve-fitting method was used, and values of $x = 0.41$ and 0.27 respectively, were obtained. It has been remarked upon before [43] that the peak-shift method often gives higher values of x than does curve-fitting, but it is interesting to consider why this might be so.

Consider first the data of Hodge [38,39]. These were obtained from three sets of experiments: (i) cooling at 40, 20, 10 and 5 K min^{-1} and then reheating at 10 K min^{-1} after no annealing; (ii) annealing for $t_a = 1$ h at about 30, 20 and 10 K below T_g; (iii) annealing at about 30 K below T_g for $t_a = 1$ h and about 16 h. The point to notice here is the amount of annealing involved, and hence the degree of nonlinearity in the response on heating in the DSC. The type (i) experiments involved no annealing at T_a, and correspond to our constant cooling rate experiments, from which Δh^* and β (but not x) are evaluated. The degree of nonlinearity in the response, roughly assessed by the magnitude of the endothermic overshoot relative to the ΔC_p step, has a maximum value of about 1.5 (Fig. 1 in Ref. [38] or Fig. 4 in Ref. [39]), is much less than that in the present annealing experiments (maximum overshoot approximately 6 for $T_a = 2000$ h, see Fig. 3), and even significantly less than in our constant cooling rate experiments (maximum $C^N_{p,u} = 2.3$, see Fig. 10). Similarly, for type (ii) and type (iii) experiments, the maximum overshoot was only about 2.1, a factor of about 3 smaller than in the present work. Thus the degree of nonlinearity in the response to Hodge's thermal histories is much less than it is here, and we therefore infer that Hodge's data are much less sensitive to the nonlinearity parameter x than are the present data. Consequently, we believe that the results from the peak-shift method are more reliable for the evaluation of x. In this respect, it is also of interest to note that the experiments of Sasabe and Moyihan [37], which are the same as those of type (i) of Hodge [38,39], extend to lower cooling rates (0.62 K min^{-1}) and hence yield larger overshoots (maximum $C^N_{p,u} \approx 2.1$) than do Hodge's experiments, and that correspondingly the value of x obtained by Sasabe and Moynihan (0.41) is closer to that obtained here.

5.4. The equilibrium state and ΔH_∞

We now turn to the question of the equilibrium enthalpy or the maximum enthalpy loss, ΔH_∞, and whether or not this may reliably be estimated for $T_a < T_g$ by extrapolation from equilibrium values at temperatures above T_g. Consider first the constant cooling rate data of Fig. 7. From these data, the dependence of the fictive temperature on cooling rate was found, from which Δh^* was evaluated. From the same data, the excess enthalpy difference between glassy states defined by the different cooling rates may also be evaluated, simply by finding the difference in area between the relevant curves. Taking the slowest cooling rate (0.5 K min^{-1}) as a reference, the excess enthalpy difference of the other glassy states relative to this, $\Delta\bar{\delta}_H$, has been plotted versus the fictive temperature difference, also relative to the reference cooling rate of 0.5 K min^{-1}, in Fig. 11. There is a reasonably good linear relationship, the slope giving a value of $\Delta C_p = 0.475$ J g^{-1} K^{-1}; this is slightly lower

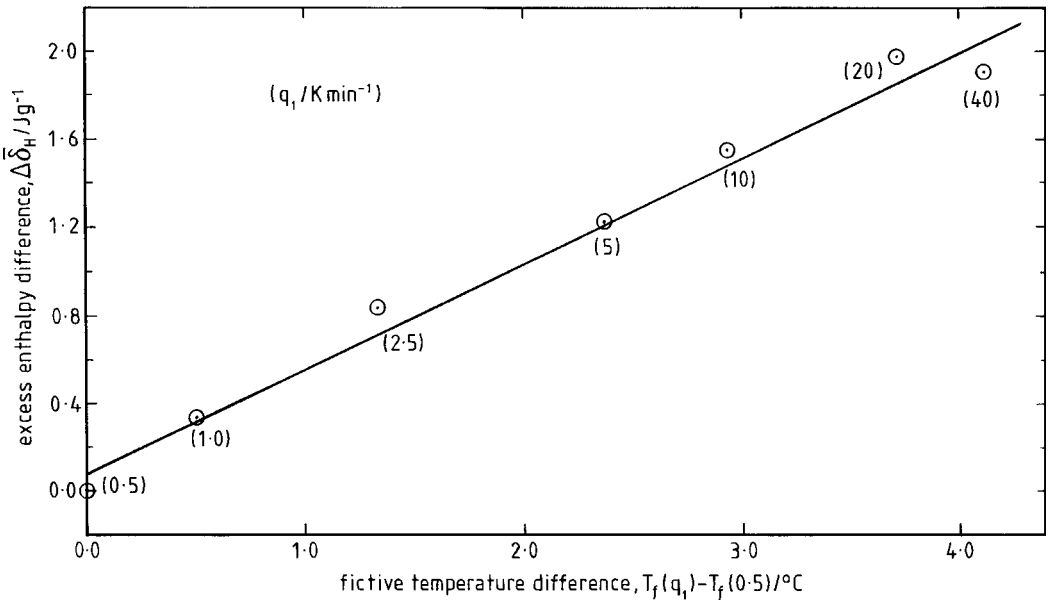

Fig. 11. Excess enthalpy difference for glassy states defined by different cooling rates, relative to a reference cooling rate of 0.5 K min^{-1}, plotted as a function of the fictive temperature difference relative to that for a cooling rate of 0.5 K min^{-1}. The cooling rates are given in brackets against each point, and the data were evaluated from the curves in Fig. 7. The straight line represents a least-squares fit to the data.

than the value obtained further above (0.505 ± 0.010 J g^{-1} K^{-1}), which could imply a small amount of upward curvature in the *H–T* plot. We conclude from this that the linear extrapolation of equilibrium values of enthalpy is a reasonable approximation down to temperatures 4 K below T_g(40 K min^{-1}), involving recovered enthalpies of up to approximately 2 J g^{-1}.

It is notable that there are already certain inconsistencies between these results and those of Cowie et al. [14]. In the latter work, T_g(40 K min^{-1}) = 42 °C, and their highest T_a = 35 °C, which is 7 °C below T_g(40 K min^{-1}). For this annealing temperature, they find $\Delta H_\infty = 1.9$ J g^{-1} which, if this corresponded to an extrapolated value from higher temperatures, would give $\Delta C_p = 0.271$ J g^{-1} K^{-1}. Although no value for ΔC_p is quoted in their paper, this would appear to be much too small.

An alternative way of comparing the present data with those of Cowie et al. [14] is to remark that in our experiments an equilibrium enthalpy difference of about 2 J g^{-1} is measured about 4 °C below T_g(40 K min^{-1}), whereas their data show approximately the same ΔH_∞ (1.9 J g^{-1}) at almost twice the ΔT below T_g(40 K min^{-1}). Since, over the rather narrow temperature interval being considered here, the effect of a small amount of curvature in the *H–T* plot would not account for this difference, we may consider two possibilities for these inconsistencies.

The first possibility is that different equilibrium states are achieved when different paths are followed, namely cooling at 40 K min^{-1} to T_a and then annealing at T_a, or cooling sufficiently slowly that equilibrium is maintained at all temperatures down to T_a. Such a possibility calls into question the meaning of an "equilibrium" state at T_a, as has been intimated by several authors [13–18], and would have profound implications for our understanding of the glass transformation process. However, before developing these implications it is essential to ensure that the hypothesis is not based upon an incorrect interpretation of the data, which could be implied by the second possibility.

This second possibility is that the extrapolated ΔH_∞ values using the CF equation (1) are not in fact the real equilibrium values. This possibility arises because it is recognised that the CF equation is only empirical and does not take into account the changes in the relaxation time occurring during isothermal relaxation, and

that as a consequence the parameter values extracted may be unreliable. Indeed, this has already been shown above to be true of the Δh^* values found by this fitting procedure, and this in itself has implications for the ΔH_∞ values.

In the CF equation (1), the value of τ is the time t_a at which the relaxation $\Delta H(t_a)$ has proceeded to within a fraction of $1/e$ of the final ΔH_∞ value:

$$\frac{\Delta H(t_a = \tau)}{\Delta H_\infty} = 1 - \frac{1}{e} \tag{15}$$

Thus too small a value of τ must involve also too small a value for ΔH_∞. We believe therefore that the CF approach consistently underestimates ΔH_∞, with the result that it appears as if the equilibrium state has been reached at ΔH_∞ values much less than the values extrapolated from equilibrium data at higher temperatures.

This possibility can be examined in some more detail by comparing the data presented here, for $T_a = 30.0\ ^\circ C$ (relative to $T_g(40\ K\ min^{-1}) = 40.0\ ^\circ C$), with those of Cowie et al. [14] for $T_a = 30.0\ ^\circ C$ (relative to $T_g(40\ K\ min^{-1}) = 42.0\ ^\circ C$), as well as with other data from the literature for experimental conditions closely corresponding to those used here. The assembled sets of data are plotted as enthalpy loss versus log (ageing time) in Fig. 12, the details of the origin of each set of data being provided in the caption.

The data obtained in our own laboratory in successive years using the same PVAc samples (open and filled rhombuses) show very good agreement. The former [44] are truncated at an ageing time of approximately 100 h for the following reason. The samples were contained in tubes of the type shown in Fig. 1 for the long annealing times, and the tubes were packed with silica gel to try and ensure that the samples remained dry. Nevertheless, for ageing times longer than some 100 h, the enthalpy loss and the peak temperature T_p both showed a reduction from the trend seen in Fig. 12, and for times longer than about 300 h there was a dramatic fall in both values. It was

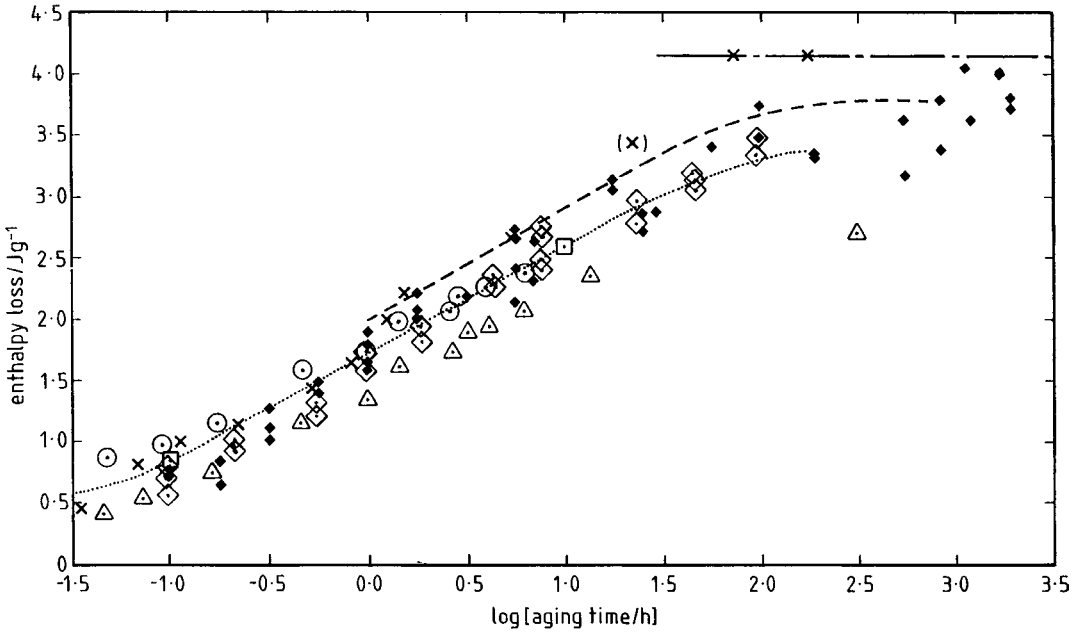

Fig. 12. Isothermal enthalpy relaxation data for the present work (filled rhombuses) and earlier work [44] on the same PVAc samples (open rhombuses) compared with other data for PVAc taken from the literature: open squares (□, two points only) and dotted line represent isothermal volume relaxation data for PVAc at 30 °C taken from Kovacs (Fig. 15 in Ref. [8]), scaled by 1.21 such that $\Delta\delta_\infty$ for volume relaxation corresponds to $\Delta H_\infty = 3.8\ J\ g^{-1}$ for enthalpy relaxation; crosses (×) taken from enthalpy relaxation data of Bair et al. [33] at 30 °C (their Fig. 11) following a quench from above T_g, with dash-dotted line indicating $\Delta H_\infty = 4.18\ J\ g^{-1}$; open circles (○) taken from Cowie et al. [35], their Table 1, for isothermal enthalpy relaxation at 30 °C following a quench from above T_g; dashed line (- - -) taken from Wang and Filisko [34], their Fig. 4 for isothermal relaxation at 30 °C following a quench from 40 °C, shifted vertically to give $\Delta H_\infty = 3.75\ J\ g^{-1}$; open triangles (△) taken from Cowie et al. [14], their Fig. 4, for $T_a = 30.0\ ^\circ C$.

surmised that this was caused by moisture penetration to the sample at these long times, and for the subsequent set of experiments, for which the data are presented in this paper, further precautions were taken to seal the opening of the tubes in addition to packing them with silica gel. It can be seen that there is no longer the dramatic drop in enthalpy loss at long times, though the increased scatter in the data is believed still to be associated with the sensitivity of the sample to moisture absorption. Nevertheless, there is a clear trend of the data approaching a limiting value even if there is some uncertainty in the value of this limit.

The data of Bair et al. [33], indicated by crosses, were obtained following a quench at 160 K min^{-1} from 70 to 30 °C. They are presented as enthalpy loss by taking their quoted value of $\Delta H_\infty = 4.18$ J g^{-1}, indicated in Fig. 12 by the dash-dotted line. The point shown in parentheses has been replotted, believed to have been incorrectly annotated in the original.

The data of Wang and Filisko [34] relate to isothermal relaxation at 30 °C following a quench from 40 °C. They are shown as the dashed line, and have been adjusted on the vertical scale such that $\Delta H_\infty = 3.75$ J g^{-1}, the average limiting value from our own data, in order to present them in the form of enthalpy loss. The open circles refer to the data of Cowie et al. [35] for isothermal relaxation at 30 °C following a quench from above T_g, while the open triangles relate to later results from the same laboratory [14]. This last set of data lies slightly below the other data, and in particular there is one data point at long times which lies significantly below the other trends, and on its own would suggest a limiting enthalpy loss considerably less than is here believed to be the case.

Despite the numerous different laboratories involved in these measurements, different thermal treatments (e.g. initial temperature and quench rate) and sample details, there is apparently considerable consistency in the enthalpy relaxation behaviour in the early stages, all the data being contained within a band of width 0.6 J g^{-1} approximately. Indeed, the volume relaxation data of Kovacs [8] for PVAc quenched from 40 to 30 °C have also been included (dotted line) by scaling the relative excess volume δ by a factor of 1.21×10^3 such that $\Delta\delta_\infty$ for volume relaxation ($=3.14 \times 10^{-3}$ from Table 7 of Ref. [8]) scales to $\Delta H_\infty = 3.8$ J g^{-1}, the average limiting value here (filled rhombuses), and it is clear that the volume relaxation data in this range up to 100 h correspond closely to the enthalpy relaxation data.

Nevertheless, closer scrutiny of all these sets of data reveals significant differences, and extrapolation to limiting values is dangerous. For example, the volume relaxation data were plotted here by assuming an equivalent enthalpy loss of 3.8 J g^{-1}, a value that would not seem immediately obvious from a simple visual inspection of the data. Interestingly, this also seems to confirm that quite different timescales may apply to volume and enthalpy relaxation, as has been suggested before [4–6], though the present results are unusual in that the enthalpy appears to reach equilibrium more rapidly than does the volume at the same temperature.

More importantly in the present context, however, are the limiting values of the enthalpy loss. Our own data show a limiting value of about 3.75 J g^{-1}, albeit with some scatter, which is similar to the limiting values from the experiments of both Bair et al. [33] and Wang and Filisko [34]. It is pertinent, however, to compare this with the value that would be obtained by a linear extrapolation. This latter would give $\Delta H_\infty = \Delta C_p\, \Delta T = 4.49 \pm 0.09$ J g^{-1} with our measured value for ΔC_p and with $\Delta T = 8.9$ °C below T_g(10 K min^{-1}), which is clearly greater than the limiting value in Fig. 12, even allowing for an uncertainty of ± 0.25 J g^{-1}. The difference, however, which has a mean value of about 0.75 J g^{-1}, is not so great as to require a new interpretation of the equilibrium or limiting states, for the following reasons.

First, it can be seen from Fig. 4 that an enthalpy loss of about 0.5 J g^{-1}, which is of the order of magnitude of the difference discussed above, occurs within less than 6 min of annealing time at 30 °C. Thus even a short stabilisation time in the DSC at the start of the annealing period and immediately following the controlled cooling rate (an inevitable part of the experimental procedure which might have a duration of some 2 min) can involve an enthalpy loss of the order of 0.3 J g^{-1}, which would not be accounted for in the "ideal" $\Delta H_\infty = \Delta C_p\, \Delta T$ calculation.

Second, it is possible that a difference of the order of 0.75 J g^{-1} in ΔH_∞ values could be explained by a small amount of upward curvature in the equilibrium H–T line, as would be anticipated if C_{pl} increased with increasing temperature, as is commonly observed. We

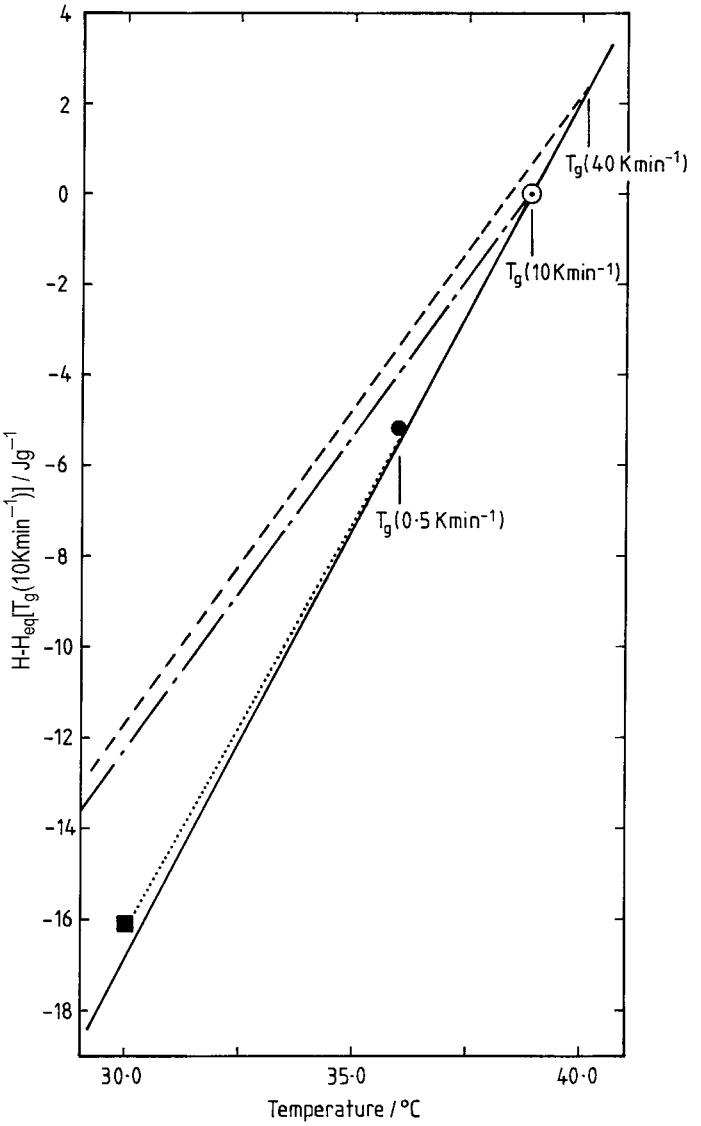

Fig. 13. Plot of enthalpy, relative to its value in equilibrium at T_g(10 K min^{-1}), as a function of temperature. The dashed and dash-dotted lines represent glassy lines for cooling rates 40 and 10 K min^{-1}, respectively, while the full line represents equilibrium. The slopes of these lines are taken from Kovacs [8]. The T_g values for the different cooling rates are found from Figs. 9 and 11. The filled circle represents the equilibrium enthalpy at T_g(0.5 K min^{-1}) determined experimentally by extrapolation from faster cooling rates. The filled square represents the equilibrium enthalpy determined experimentally from isothermal annealing experiments at 30 °C. The dotted line is the representation of Eq. (17), the extrapolated equilibrium curve according to Sasabe and Moynihan [37].

have already seen from Fig. 11 that the excess enthalpies for different cooling rates correspond to a value of $\Delta C_p = 0.475$ J g^{-1} K^{-1}, slightly less than our earlier value of 0.505 J g^{-1} K^{-1}, over the temperature range from T_g(40 K min^{-1}) = 40.1 °C to T_g(0.5 K min^{-1}) = 36.0 °C, and it was noted that this was consistent with a small amount of upward curvature of the equilibrium line. This is best illustrated by reference to Fig. 13, where the enthalpy relative to its equilibrium value at T_g(10 K min^{-1}) is plotted as a function of temperature. The (constant) slopes of the glassy lines corresponding to cooling rates of 40 and 10 K min^{-1} and of

the equilibrium line have been drawn using values for C_{pg} and C_{pl}, respectively, taken from Table 1 in Ref. [8]. The excess enthalpy at $T_g(0.5\,\mathrm{K\,min^{-1}})$ after cooling at $40\,\mathrm{K\,min^{-1}}$ is calculated from $\Delta H_\infty = \Delta C_p\,\Delta T$ as $2.1\,\mathrm{J\,g^{-1}}$, using $\Delta T = T_g(40\,\mathrm{K\,min^{-1}}) - T_g(0.5\,\mathrm{K\,min^{-1}}) = 40.1 - 36.0\,^\circ\mathrm{C}$, and is represented as the difference between the dashed and full lines at $T_g(0.5\,\mathrm{K\,min^{-1}})$ in Fig. 13. The corresponding experimentally measured excess enthalpy is $1.9\,\mathrm{J\,g^{-1}}$ (Fig. 11), implying an equilibrium enthalpy state as indicated by the filled circle, which would be consistent with a small amount of upward curvature in the equilibrium line.

At 30 °C, in our isothermal annealing experiments, the initial cooling rate was $10\,\mathrm{K\,min^{-1}}$ and the limiting excess enthalpy was found as $3.75 \pm 0.25\,\mathrm{J\,g^{-1}}$ with respect to this cooling rate, implying an average equilibrium state as indicated by the filled square. This again is consistent with only a small amount of upward curvature of the equilibrium line. In fact, this upward curvature can be deduced from the temperature dependence of the equilibrium heat capacity quoted by Sasabe and Moynihan [37] for PVAc in the temperature range from 330 to 340 K, i.e. well above T_g. These authors give (their Eq. (1b)):

$$C_{pl} = 1.183 + 0.002115T \tag{16}$$

when the units of C_p are converted to $\mathrm{J\,g^{-1}\,K^{-1}}$ and the temperature is in Kelvin. Integrating this to give the temperature dependence of the enthalpy, and setting the constant of integration such that the enthalpy is zero at $T_g(10\,\mathrm{K\,min^{-1}}) = 38.9\,^\circ\mathrm{C}$, yields the following equation for the equilibrium enthalpy H_{eq} (in $\mathrm{J\,g^{-1}}$) as a function of temperature:

$$H_{eq} = 1.183T + 0.0010575T^2 - 471.86 \tag{17}$$

This equation is plotted in Fig. 13 as the dotted line, from which it can be seen that our experimentally measured enthalpy values at 30 °C (filled square) and at $T_g(0.5\,\mathrm{K\,min^{-1}}) = 36.0\,^\circ\mathrm{C}$ (filled circle), which deviate from the linearly extrapolated H–T line, fall almost exactly on the extrapolation of the equilibrium data of Sasabe and Moynihan [37].

Third, the equation $\Delta H_\infty = \Delta C_p\,\Delta T$ assumes that the asymptotic glassy regime has been achieved, on cooling, by the time the annealing temperature T_a is reached. If the width of the transition interval was 20 K, a not unreasonable value, and the interval was centred on $T_g(10\,\mathrm{K\,min^{-1}})$, then an annealing temperature of only 8.9 K below $T_g(10\,\mathrm{K\,min^{-1}})$ would not be within the asymptotic regime. Thus there would be an extra amount of excess enthalpy to be recovered experimentally, which is not included in the $\Delta C_p\,\Delta T$ calculation.

All of these possibilities combine to indicate that our present data are consistent with the isothermal enthalpy relaxation at approximately 10 K below T_g approaching an equilibrium state that is the same as that extrapolated (not necessarily linearly) from equilibrium states at higher temperatures. Thus, for PVAc under these conditions, it is not necessary to invoke ideas of a limiting state different from the extrapolated equilibrium state.

6. Conclusions

From isothermal enthalpy relaxation experiments at an annealing temperature of 30 °C and from experiments to determine the cooling rate dependence of the fictive temperature, the relaxation parameters for PVAc have been determined by the peak-shift method as $\Delta h^* = 805\,\mathrm{kJ\,mol^{-1}}$, $x = 0.44 \pm 0.02$ and $0.456 < \beta < 0.6$. These values for Δh^* and β are shown to compare reasonably well with literature values obtained by the curve-fitting technique, whereas some differences are seen in respect of the nonlinearity parameter x. It is argued that these latter differences result from inadequate nonlinearity in the curve-fitting experiments, and that the peak-shift method, involving annealing times up to 2000 h or so, is more sensitive to nonlinearity and therefore likely to give a more reliable value for x.

The results are compared also with those obtained from fitting isothermal relaxation data by the Cowie–Ferguson (CF) equation, and significant discrepancies are found, not only in the above parameter values but also in the estimated limiting values of enthalpy loss in equilibrium, ΔH_∞. It is argued that these discrepancies arise from the omission of nonlinearity from the CF equation, which results in a consistent underestimation of ΔH_∞. In contrast to the results obtained by the CF approach, we find here that our ΔH_∞ values are consistent with the assumption that the equilibrium state below T_g may be approximated by an extrapolation (not necessarily linear, but anyway with only little

curvature) from equilibrium states above T_g, at least over the somewhat limited temperature interval of approximately 10 K used here. Hence, for PVAc under these circumstances, we believe that it is not necessary to invoke the idea of a limiting state different from the extrapolated equilibrium state.

References

[1] L.C.E. Struik, Physical Aging in Amorphous Polymers and Other Materials, Elsevier, Amsterdam, 1978.
[2] I.M. Hodge, J. Non-Cryst. Solids 169 (1994) 211.
[3] J.M. Hutchinson, Prog. Polym. Sci. 20 (1995) 703.
[4] S.E.B. Petrie, J. Polym. Sci. Pt. A-2 10 (1972) 1255.
[5] J. Perez, J.Y. Cavaille, R. Diaz Calleja, J.L. Gómez Ribelles, M. Montleón Padras, A. Ribes Greus, Makromol. Chem. 192 (1991) 2141.
[6] M. Delin, R.W. Rychwalski, J. Kubat, C. Klason, J.M. Hutchinson, Polym. Eng. Sci. 36 (1996) 2978.
[7] A.J. Kovacs, Thesis, Faculty of Science, University of Paris, 1954.
[8] A.J. Kovacs, Fortschr. Hochpolym. Forsch. 3 (1963) 394.
[9] J.M. Hutchinson, M. Ruddy, Makromol. Chem., Makromol. Symp. 27 (1989) 319.
[10] J.M. Hutchinson, in: R.N. Haward, R.J. Young (Eds.), The Physics of Glassy Polymers, 2nd Edition, Chapman & Hall, London, 1997 (Chapter 3).
[11] J.M.G. Cowie, R. Ferguson, Macromolecules 22 (1989) 2307.
[12] J.M.G. Cowie, R. Ferguson, Polymer 34 (1993) 2135.
[13] A. Brunacci, J.M.G. Cowie, R. Ferguson, I.J. McEwen, Polymer 38 (1997) 865.
[14] J.M.G. Cowie, S. Harris, I.J. McEwen, J. Polym. Sci. Polym. Phys. Ed. 35 (1997) 1107.
[15] J.L. Gómez Ribelles, M. Montleón Pradas, Macromolecules 28 (1995) 5867.
[16] J.L. Gómez Ribelles, M. Montleón Pradas, J. Más Estellés, A. Vidaurre Garayo, F. Romero Colomer, J.M. Meseguer Dueñas, Polymer 38 (1997) 963.
[17] J.M. Meseguer Dueñas, A. Vidaurre Garayo, F. Romero Colomer, J. Más Estellés, J.L. Gómez Ribelles, M. Montleón Pradas, J. Polym. Sci. Polym. Phys. Ed. 35 (1997) 2201.
[18] S. Monserrat, J.L. Gómez Ribelles, J.M. Meseguer, Polymer 39 (1998) 3801.
[19] I.M. Hodge, J.M. O'Reilly, Polymer 33 (1992) 4883.
[20] A.Q. Tool, J. Am. Ceram. Soc. 29 (1946) 240.
[21] M. Delin, R.W. Rychwalski, J.M. Hutchinson, J. Kubát, C. Klason, Ann. Trans. Nordic Rheol. Soc. 3 (1995) 64.
[22] M. Delin, R.W. Rychwalski, J.M. Hutchinson, J. Kubát, in: M. Giordano, D. Leporini, M.P. Tosi (Eds.), Non-equilibrium Phenomena in Supercooled Fluids, Glasses and Amorphous Materials, World Scientific, Singapore, 1996, p. 285.
[23] R.W. Rychwalski, J. Vernel, M. Delin, J. Kubát, J.M. Hutchinson, A.V. Vannikov, V. Pelíšek, in: Proceedings of the Third International Discussion Meeting on Relaxation in Complex Systems, Vigo, Spain, June 30–July 11, 1997.
[24] A.J. Kovacs, J.J. Aklonis, J.M. Hutchinson, A.R. Ramos, J. Polym. Sci. Polym. Phys. Ed. 17 (1979) 1097.
[25] A.R. Ramos, J.M. Hutchinson, A.J. Kovacs, J. Polym. Sci. Polym. Phys. Ed. 22 (1984) 1655.
[26] J.M. Hutchinson, Lect. Notes Phys. 277 (1987) 172.
[27] J.M. Hutchinson, A.J. Kovacs, in: P.H. Gaskell (Ed.), The Structure of Non-crystalline Solids, Taylor & Francis, London, 1977, p. 167.
[28] O.S. Narayanaswamy, J. Am. Ceram. Soc. 54 (1971) 491.
[29] C.T. Moynihan, A.J. Easteal, M.A. De Bolt, J. Tucker, J. Am. Ceram. Soc. 59 (1976) 12.
[30] J.M. Hutchinson, M. Ruddy, J. Polym. Sci. Polym. Phys. Ed. 28 (1990) 2127.
[31] M.J. Richardson, N.G. Savill, Polymer 16 (1975) 753.
[32] Yu.A. Sharonov, M.V. Volkenshtein, in: E.A. Porai-Koshits (Ed.), The Structure of Glass, Vol. 6, Consultants Bureau, New York, 1966, p. 62.
[33] H.E. Bair, G.E. Johnson, E.W. Anderson, S. Matsuoka, Polym. Eng. Sci. 21 (1981) 930.
[34] C.-H. Wang, F.E. Filisko, Polym. Mater. Sci. Eng. 62 (1990) 782.
[35] J.M.G. Cowie, S. Elliott, R. Ferguson, R. Simha, Polym. Commun. 28 (1987) 298.
[36] J.E. McKinney, R. Simha, Macromolecules 9 (1976) 430.
[37] H. Sasabe, C.T. Moynihan, J. Polym. Sci. 16 (1978) 1447.
[38] I.M. Hodge, Macromolecules 16 (1983) 898.
[39] I.M. Hodge, Macromolecules 20 (1987) 2897.
[40] J.M. Hutchinson, M. Ruddy, J. Polym. Sci. Polym. Phys. Ed. 26 (1998) 2341.
[41] V.P. Privalko, S.S. Demchenko, Yu.S. Lipatov, Macromolecules 19 (1986) 901.
[42] J.J. Tribone, J.M. O'Reilly, J. Greener, Macromolecules 19 (1986) 1732.
[43] J.M. Hutchinson, Polym. Int. 47 (1998) 56.
[44] K. Lee, Unpublished data, BEng Final Year Project, University of Aberdeen, 1997.